

# Input polarization-independent polarization-sensitive optical coherence tomography using a depolarizer

Cite as: Rev. Sci. Instrum. **91**, 043706 (2020); <https://doi.org/10.1063/5.0001871>

Submitted: 20 January 2020 . Accepted: 25 March 2020 . Published Online: 10 April 2020

Shivani Sharma,  Georg Hartl,  Sheeza K. Naveed,  Katharina Blessing,  Gargi Sharma, and  Kanwarpal Singh



View Online



Export Citation



CrossMark

## ARTICLES YOU MAY BE INTERESTED IN

[An electrochemical cell for 2-dimensional surface optical reflectance during anodization and cyclic voltammetry](#)



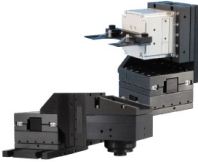
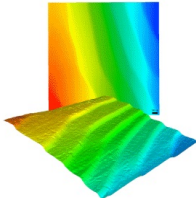
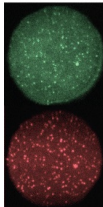
Review of Scientific Instruments **91**, 044101 (2020); <https://doi.org/10.1063/1.5133905>

[X-ray diffraction at the National Ignition Facility](#)

Review of Scientific Instruments **91**, 043902 (2020); <https://doi.org/10.1063/1.5129698>

[The energy-resolved neutron imaging system, RADEN](#)

Review of Scientific Instruments **91**, 043302 (2020); <https://doi.org/10.1063/1.5136034>

 <b>MCL</b> MAD CITY LABS INC. <a href="http://www.madcitylabs.com">www.madcitylabs.com</a>	<p>Nanopositioning Systems</p> 	<p>Modular Motion Control</p> 	<p>AFM and NSOM Instruments</p> 	<p>Single Molecule Microscopes</p> 
---	--	--	---	--

# Input polarization-independent polarization-sensitive optical coherence tomography using a depolarizer

Cite as: Rev. Sci. Instrum. 91, 043706 (2020); doi: 10.1063/5.0001871

Submitted: 20 January 2020 • Accepted: 25 March 2020 •

Published Online: 10 April 2020



View Online



Export Citation



CrossMark

Shivani Sharma,<sup>1,2</sup> Georg Hartl,<sup>1,2</sup>  Sheeza K. Naveed,<sup>1,2</sup>  Katharina Blessing,<sup>1</sup>  Gargi Sharma,<sup>1</sup>   
and Kanwarpal Singh<sup>1,a)</sup> 

## AFFILIATIONS

<sup>1</sup>Max Planck Institute for the Science of Light, Staudtstr. 2, 91058 Erlangen, Germany

<sup>2</sup>Department of Physics, Friedrich-Alexander Universität Erlangen-Nürnberg, Staudtstr. 7, 91058 Erlangen, Germany

<sup>a)</sup>Author to whom correspondence should be addressed: [kanwarpal.singh@mpl.mpg.de](mailto:kanwarpal.singh@mpl.mpg.de)

## ABSTRACT

Polarization-sensitive optical coherence tomography is gaining attention because of its ability to diagnose certain pathological conditions at an early stage. The majority of polarization-sensitive optical coherence tomography systems require a polarization controller and a polarizer to obtain the optimal polarization state of the light at the sample. Such systems are prone to misalignment since any movement of the optical fiber normally coupled to the light source will change the polarization state of the incident beam. We propose and demonstrate an input polarization-independent polarization-sensitive optical coherence tomography system using a depolarizer that works for any input polarization state of the light source. The change in the optical power at the sample for arbitrary input polarized light for the standard polarization-sensitive optical coherence tomography system was found to be approximately 84% compared to 9% for our proposed method. The developed system was used to measure the retardance and optical axis orientation of a quarter-wave plate and the obtained values matched closely to the expectation. To further demonstrate the capability of measuring the birefringent properties of biological samples, we also imaged the nail bed. We believe that the proposed system is a robust polarization-sensitive optical coherence tomography system and that it will improve the diagnostic capabilities in clinical settings.

© 2020 Author(s). All article content, except where otherwise noted, is licensed under a Creative Commons Attribution (CC BY) license (<http://creativecommons.org/licenses/by/4.0/>). <https://doi.org/10.1063/5.0001871>

## I. INTRODUCTION

Optical coherence tomography (OCT), first demonstrated in 1991,<sup>1</sup> is a powerful imaging technique to acquire cross-sectional images with a depth resolution of a few micrometers. OCT is an interferometric imaging technique that measures the backscattering of the sample to obtain two-dimensional and three-dimensional images. Applications are found in several fields of medical imaging such as coronary artery,<sup>2</sup> ophthalmology,<sup>3</sup> and gastroenterology.<sup>4</sup>

In pathological studies, standard OCT is good at detecting morphological changes, but unfortunately such changes only present themselves at an advanced stage of the disease. Several pathological conditions such as cancer can be detected at an early stage

by measuring the birefringent properties of the tissue.<sup>5</sup> To analyze the additional details of the polarization information carried by the scattered light from the sample, an extended form of OCT, called polarization-sensitive optical coherence tomography (PS-OCT), has been developed.<sup>6–9</sup>

In PS-OCT systems, two images of the sample, one for each orthogonal polarization state, are acquired. These images are further analyzed to extract the birefringence and reflectance properties of the tissue. PS-OCT has been applied in several fields of biomedical imaging, which includes human retinal imaging,<sup>10</sup> endobronchial imaging,<sup>11</sup> esophagus imaging,<sup>12</sup> and brain tumor imaging.<sup>13</sup>

Several variants of PS-OCT have been developed and demonstrated up to today. Two major branches of PS-OCT systems exist at

present: spectrometer-based PS-OCT systems<sup>14,15</sup> and swept-source based PS-OCT systems.<sup>16</sup> Spectrometer-based systems can be further divided into two categories: single-camera based<sup>14,15</sup> and multiple cameras<sup>10</sup> based. Single camera-based systems can be built at a lower cost than multiple camera-based systems. Camera-based systems offer better resolution as such systems can be operated at shorter wavelength, but swept-source based PS-OCT systems offer deeper imaging depths with a better signal-to-noise ratio. Since imaging depth and sensitivity roll-off is better<sup>17</sup> in swept-source PS-OCT systems as compared to camera-based systems, such systems can be easily used to acquire tissue images in orthogonal polarization states simultaneously.

In the majority of the PS-OCT systems,<sup>6-9,16</sup> the laser light is first polarized in a fixed plane using a combination of a polarization controller and a polarizer. Then, this light is further manipulated using various polarizing and nonpolarizing components to acquire the desired input state for imaging. Once the optimal polarization state is achieved in the system, the optical fiber is fixed to minimize the changes in polarization states which can occur if the fiber is bent or twisted. Furthermore, any change in the input polarization state would require a realignment of the system. This is particularly challenging in clinical settings where the operator has limited experience with such systems.

In this work, we present a swept-source based input polarization-independent polarization-sensitive optical coherence tomography (IPIPS-OCT) setup. Our system uses a depolarizer and a polarizer to control the polarization, which makes the system much simpler and easier to use. The performance of the system was tested against a quarter-wave plate, providing known birefringent optical properties. Furthermore, a nail bed from a healthy volunteer was imaged, and its cumulative retardance and optical axis orientation was measured to confirm the potential of our system for imaging biological samples.

## II. METHODS

The experimental setup for IPIPS-OCT is illustrated in Fig. 1. A commercial swept-source OCT engine (Axsun Technologies, North Billerica, MA, USA) provides the laser source and a data processing unit. It emits laser light with a sweep rate of 100 kHz, a central wavelength of 1310 nm, a scan range of 140 nm, and an output power of 24 mW.

The light from the laser source was coupled into the system via a fiber (SMF-28) and a lens (L1). A depolarizer (DP, Thorlabs, DPP25-C, Newton, NJ, USA) was used after the lens L1 to convert the partially polarized light from the light source into depolarized light. The beam waist ( $1/e^2$ ) at the depolarizer was measured to be 1.1 mm. A polarizing beam splitter (Thorlabs, PBS104, Newton, NJ, USA), placed behind the depolarizer, acted as a linear polarizer and transmitted horizontally polarized (with respect to the lab frame) light. A non-polarizing (50/50) beam splitter (NPBS1, Thorlabs, BS012, Newton, NJ, USA) split the beam into the sample and reference arm. The light signal in the reference arm was further divided into two parts using another non-polarizing (50/50) beamsplitter (NPBS2, Thorlabs, BS012, Newton, NJ, USA). An achromatic quarter-wave plate (QWP1, Thorlabs, AQWP10M-1600, Newton, NJ, USA) was inserted in one of the reference arms

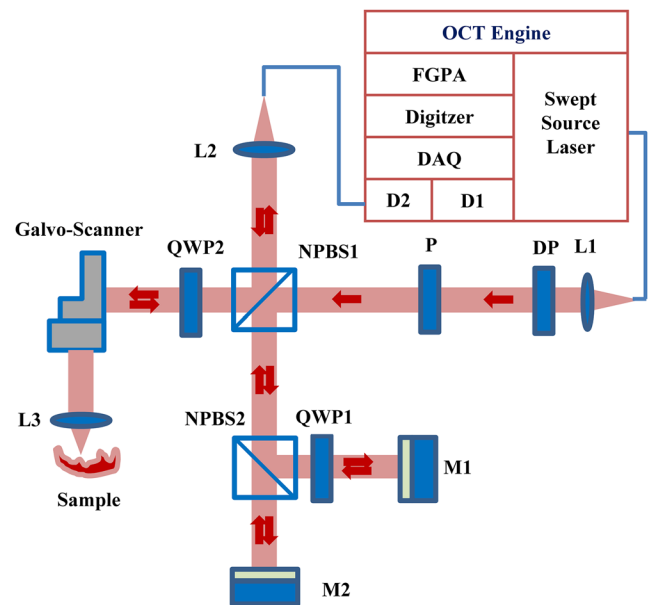


**FIG. 1.** Schematics of the IPIPS-OCT system. Lens (L), depolarizer (DP), polarizer (P), non-polarizing beam splitter (NPBP), quarter wave plate (QWP), mirror (M), detector (D), data acquisition card (DAQ), and field programmable gate arrays (FPGAs).

and rotated to obtain orthogonally polarized light in relation to the second reference signal. The optical path difference between the two reference mirrors, M1 and M2, and the sample was adjusted until the horizontal and vertical polarized sample images were separated. This allows displaying both images within the imaging range of the system.

In the sample arm, another achromatic quarter-wave plate (QWP2, Thorlabs, AQWP10M 1600, Newton, NJ, USA) was used to convert the incoming light into circularly polarized light. A two-axis Galvo scanner (Thorlabs, GVS012, Newton, NJ, USA) was used for lateral scanning of the sample.

Light reflected from the two reference mirrors and the sample was recombined and coupled to a SMF after NPBS1 using a lens (L2). The combined signal was detected using an integrated photodiode (D2, 3 dB bandwidth = 267.96 MHz) within the OCT engine. The signal from the detector was digitized using an on-board 12 bit, 500 MS/s digitizer. The obtained data of one sweep were transferred to a built-in field-programmable gate array (FPGA) module, which applies a Hamming window function and a subsequent inverse Fourier transform, resulting in axial scans. 2500 axial scans were collected to form a B-scan of the sample and transferred to the host computer via an Ethernet cable. On the host computer, a custom-designed LabView software was used to collect the image data from the OCT engine. The LabView software only acted as the interface between the OCT engine and host workstation and was responsible for the acquisition of the images from the FPGA module, displaying the images on the screen and then saving them to the hard drive on the host workstation.

As the two reference signals were delayed with respect to each other, this generated depth encoded images within one B-scan of the sample. The images were termed horizontal and vertical channels corresponding to the images generated from the interference of the light reflected from the sample with the reflection from mirrors M2 and M1, respectively. Parameters such as reflectivity  $R(z)$ , single pass retardance  $\delta(z)$ , and optical axis orientation  $\theta(z)$  in the axial direction of the sample can be calculated using the following formulas:<sup>10,18</sup>

$$R(z) = \sqrt{A_H^2(z) + A_V^2(z)}, \quad (1)$$

$$\delta(z) = \tan^{-1} \left[ \frac{A_H(z)}{A_V(z)} \right], \quad (2)$$

$$\theta(z) = \frac{180^\circ - \Delta\phi(z)}{2}, \quad (3)$$

where  $A_H(z)$  is the amplitude of the horizontal channel,  $A_V(z)$  is the amplitude of the vertical channel, and  $\phi(z)$  is the phase difference between the horizontal channel and the vertical channel.

The data post-processing for our system involved the following steps:

1. Horizontal and vertical polarization images were separated into individual images.
2. All zeros in the vertical polarization channel image were replaced with the mean of the noise floor. This helps to avoid undefined values in the retardance calculation.
3. Finally, sample reflectivity, retardance, and optical axis orientation were calculated using Eqs. (1)–(3), respectively.

### III. RESULTS

Our developed system had an axial resolution of approximately  $6.8 \mu\text{m}$ , a lateral resolution of  $50 \mu\text{m}$ , a sensitivity of 102 dB (1 dB drop-off at 5 mm), and an imaging range of 1.5 mm for both the horizontal and vertical channels. It should be noted that, although the full imaging range of the system was 5 mm, only 3 mm was used to exclude some fixed noise lines introduced by the optical components in the system. The imaging speed of the system was 100 000 axial lines (A-lines) per second and limited by the laser sweeping rate.

To demonstrate the effect of the input polarization, the fiber from the laser source was mounted on a manual polarization controller. The polarization of the light from the light source was changed continuously, and the optical power with and without the depolarizer was measured after polarization using a power meter (Thorlabs, PM400). These measurements are shown in Fig. 2. For a conventional PS-OCT (without depolarizer), the maximum power change was found to be approximately 84% of the input power. With the IPIPS system, we reduced the power fluctuations drastically to approximately 9%.

To test the performance of the system regarding the measurement of the polarization properties, a mirror was used as a sample, and a quarter-wave plate was inserted between the sample mirror and QWP2. The quarter-wave plate in front of the sample mirror

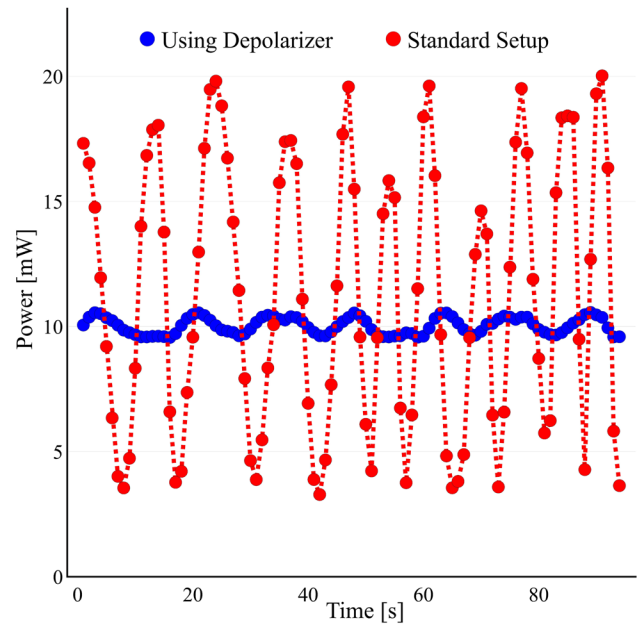


FIG. 2. Change in optical power after polarization for a conventional PS-OCT system and the IPIPS-OCT system.

was rotated between zero and  $180^\circ$ , which is equivalent to introducing a single pass retardance of  $90^\circ$  and a change in the optical axis orientation of  $180^\circ$ . The obtained retardance values and wrapped values of optical axis orientation when the quarter-wave plate was

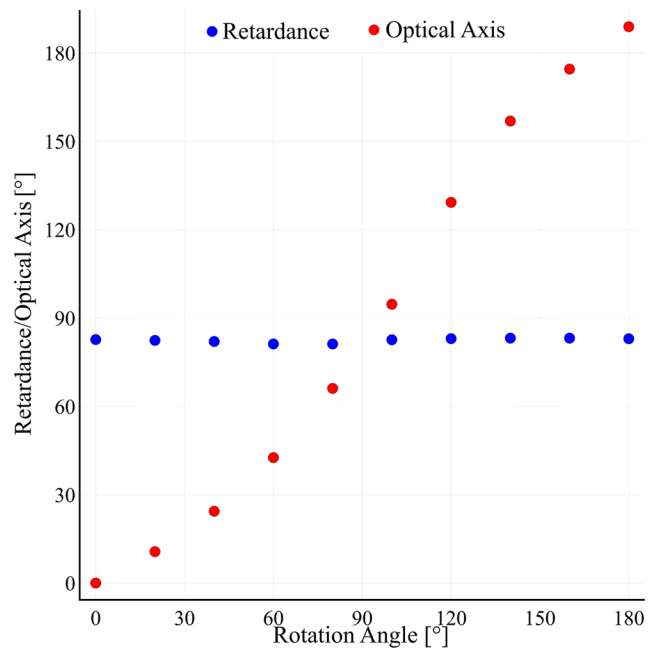
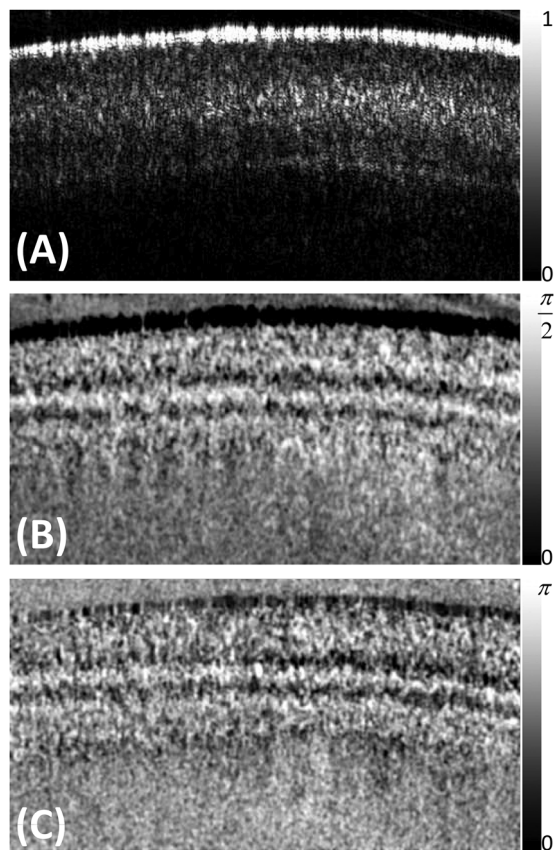


FIG. 3. Measured retardance and optical axis orientation for a quarter-wave plate for different rotation angles of the quarter-wave plate.



**FIG. 4.** Image of a nail bed (a) back scattered intensity image, (b) retardance image, and (c) optical axis orientation image.

rotated are shown in Fig. 3. The measured values match closely to the expected ones.

To test the ability of the designed system to measure the birefringent properties of biological samples, we measured the birefringence of the nail bed of a volunteer. The power at the sample was 5 mW. IPIPS-OCT allows the reconstruction of a conventional back scattered intensity image from both polarization channels. Additionally, the optical axis orientation image and the cumulative retardance image for the nail bed are shown in Fig. 4.

#### IV. DISCUSSION AND CONCLUSION

Limitations of our technique include inferior spatial resolution and a decreased sensitivity as compared to PS-OCT systems that do not use a depolarizer. As the depolarizer slightly displaces the two polarization states spatially, it reduces the spatial resolution of the system. In our system, the spatial resolution changed from 30  $\mu\text{m}$  to 50  $\mu\text{m}$ . Because of the combined effect of spatial resolution and phase variation in the beam, the sensitivity dropped by 4 dB when using the depolarizer as compared to the system without a depolarizer. Another limitation of the IPIPS-OCT configuration as compared to the standard PS-OCT system is that approximately half

of the input light is lost after polarization in the system, whereas in standard PS-OCT systems, the polarization of the input light can be aligned with the axis of the polarizer to allow full input power to pass through if the laser light is completely polarized. However, with today's powerful light sources, it should not be a major limitation as even after losing half of the power, one should be able to get sufficient power at the sample for tissue imaging with high sensitivity.

To conclude, we have developed a depolarizer based robust polarization-sensitive optical coherence tomography system that makes the polarization controller and multiple alignment obsolete. Thus, it is independent of changing input polarization states of the laser delivery.

Most of the PS-OCT systems can be easily converted to our design just by using a depolarizer in the system. Our setup enables a fast and robust way to achieve results with the same quality as a conventional PS-OCT setup. After the initial alignment, no more changes in the setup are required. This is an important step to foster the transfer of PS-OCT to heavily changing environments as needed for portable clinical applications.

#### AUTHOR'S CONTRIBUTIONS

S. Sharma and G. Hartl contributed equally to this work.

#### ACKNOWLEDGMENTS

This work was financially supported by the Max Planck Society. G. Sharma would like to thank Professor Jochen Guck for supporting her research.

#### REFERENCES

- <sup>1</sup>D. Huang, E. Swanson, C. Lin, J. Schuman, W. Stinson, W. Chang, M. Hee, T. Flotte, K. Gregory, C. Puliafito, and J. G. Fujimoto, "Optical coherence tomography," *Science* **254**, 1178 (1991).
- <sup>2</sup>H. G. Bezerra, M. A. Costa, G. Guagliumi, A. M. Rollins, and D. I. Simon, "Intracoronary optical coherence tomography: A comprehensive review: Clinical and research applications," *JACC: Cardiovasc. Interventions* **2**, 1035 (2009).
- <sup>3</sup>J. Fujimoto and D. Huang, "The development, commercialization, and impact of optical coherence tomography—History of optical coherence tomography," *Invest. Ophthalmol. Visual Sci.* **57**, OCT1 (2016).
- <sup>4</sup>T.-H. Tsai, G. J. Fujimoto, and H. Mashimo, "Endoscopic optical coherence tomography for clinical gastroenterology," *Diagnostics* **4**, 57 (2014).
- <sup>5</sup>N. Gladkova, O. Streltsova, E. Zagaynova, E. Kiseleva, V. Gelikonov, G. Gelikonov, M. Karabut, K. Yunusova, and O. Evdokimova, "Cross-polarization optical coherence tomography for early bladder-cancer detection: Statistical study," *J. Biophotonics* **4**, 519 (2011).
- <sup>6</sup>Y. Yasuno, M.-J. Ju, Y. J. Hong, S. Makita, Y. Lim, and M. Yamanari, "Jones matrix based polarization sensitive optical coherence tomography," in *Optical Coherence Tomography: Technology and Applications*, edited by W. Drexler and J. G. Fujimoto (Springer International Publishing, Cham, 2015), p. 1137.
- <sup>7</sup>B. Hyle Park, M. C. Pierce, B. Cense, and J. F. de Boer, "Jones matrix analysis for a polarization-sensitive optical coherence tomography system using fiber-optic components," *Opt. Lett.* **29**, 2512 (2004).
- <sup>8</sup>M. J. Ju, Y.-J. Hong, S. Makita, Y. Lim, K. Kurokawa, L. Duan, M. Miura, S. Tang, and Y. Yasuno, "Advanced multi-contrast Jones matrix optical coherence tomography for Doppler and polarization sensitive imaging," *Opt. Express* **21**, 19412 (2013).

- <sup>9</sup>P. Sharma, Y. Verma, K. D. Rao, and P. K. Gupta, "Single mode fiber based polarization sensitive optical coherence tomography using a swept laser source," *J. Opt.* **13**, 115301 (2011).
- <sup>10</sup>M. Pircher, C. K. Hitzenberger, and U. Schmidt-Erfurth, "Polarization sensitive optical coherence tomography in the human eye," *Prog. Retinal Eye Res.* **30**, 431 (2011).
- <sup>11</sup>J. Li, F. Feroldi, J. de Lange, J. M. A. Daniels, K. Grünberg, and J. F. de Boer, "Polarization sensitive optical frequency domain imaging system for endobronchial imaging," *Opt. Express* **23**, 3390 (2015).
- <sup>12</sup>Z. Wang, H.-C. Lee, O. O. Ahsen, B. Lee, W. Choi, B. Potsaid, J. Liu, V. Jayaraman, A. Cable, M. F. Kraus, K. Liang, J. Hornegger, and J. G. Fujimoto, "Depth-encoded all-fiber swept source polarization sensitive OCT," *Biomed. Opt. Express* **5**, 2931 (2014).
- <sup>13</sup>Y. Li, K. Chiu, X. Liu, T. Hsiao, G. Zhao, S. Li, C. Lin, and C. Sun, "Polarization-sensitive optical coherence tomography for brain tumor characterization," *IEEE J. Sel. Top. Quantum Electron.* **25**, 1 (2019).
- <sup>14</sup>B. Baumann, E. Götzinger, M. Pircher, and C. K. Hitzenberger, "Single camera based spectral domain polarization sensitive optical coherence tomography," *Opt. Express* **15**, 1054 (2007).
- <sup>15</sup>C. Fan and G. Yao, "Single camera spectral domain polarization-sensitive optical coherence tomography using offset B-scan modulation," *Opt. Express* **18**, 7281 (2010).
- <sup>16</sup>M. K. Al-Qaisi and T. Akkin, "Swept-source polarization-sensitive optical coherence tomography based on polarization-maintaining fiber," *Opt. Express* **18**, 3392 (2010).
- <sup>17</sup>B. Potsaid, B. Baumann, D. Huang, S. Barry, A. E. Cable, J. S. Schuman, J. S. Duker, and J. G. Fujimoto, "Ultrahigh speed 1050 nm swept source/Fourier domain OCT retinal and anterior segment imaging at 100,000 to 400,000 axial scans per second," *Opt. Express* **18**, 20029 (2010).
- <sup>18</sup>M. R. Hee, D. Huang, E. A. Swanson, and J. G. Fujimoto, "Polarization-sensitive low-coherence reflectometer for birefringence characterization and ranging," *J. Opt. Soc. Am. B* **9**, 903 (1992).